Supplemental Material

Browning of human adipocytes requires KLF11 and reprogramming of PPARγ super-enhancers

Anne Loft,[1] Isabel Forss,[1,8] Majken S. Siersbæk,[1,8], Søren F. Schmidt,[1] Ann-Sofie B. Larsen,[1] Jesper G. S. Madsen,[1,2] Didier F. Pisani,[3,4,5] Ronni Nielsen,[1] Mads M. Aagaard,[1] Angela Mathison,[6] Matt J. Neville,[7] Raul Urrutia,[6] Fredrik Karpe,[7] Ez-Zoubir Amri,[3,4,5] Susanne Mandrup[1]

[1]Department of Biochemistry and Molecular Biology, University of Southern Denmark, DK-5230 Odense M, Denmark; [2]NNF Center for Basic Metabolic Research, University of Copenhagen, DK-2200 Copenhagen, Denmark; [3]UMR 7277, Centre National de la Recherche Scientifique,[4]U1091, Institut National de la Santé et de la Recherche Médicale, [5]Institute of Biology Valrose, University Nice Sophia Antipolis, 06100 Nice, France; [6]Laboratory of Epigenetics and Chromatin Dynamics, Mayo Clinic, Rochester, Minnesota 55905, USA; [7]National Institute for Health Research, Oxford Biomedical Research Centre, OX3 7LE Oxford, United Kingdom

[8] These authors contributed equally

Corresponding author:
Susanne Mandrup (s.mandrup@bmb.sdu.dk)

Contents of Supplemental Material

Supplemental Tables and Figures

Supplemental Materials and Methods

Supplemental References

Table S1

Enrichment of metabolic pathway for brite-selective genes (1,691)

Term ID	Term	P-value	Genes in term	Target genes in term
hsa01212	Fatty acid metabolism	7.58E-12	48	24
hsa00190	Oxidative phosphorylation	1.08E-11	120	40
hsa00020	Citrate cycle (TCA cycle)	5.88E-11	30	18
hsa00280	Valine, leucine and isoleucine degradation	4.83E-10	44	21
hsa00071	Fatty acid degradation	3.70E-09	44	20
hsa00062	Fatty acid elongation	6.56E-09	23	14
hsa_M00087	β-oxidation	9.14E-09	12	10

Enrichment of metabolic pathway for white-selective genes (1,138)

Term ID	Term	P-value	Genes in term	Target genes in term
hsa00290	Valine, leucine and isoleucine biosynthesis	0.004	2	2
hsa00340	Histidine metabolism	0.009	28	6
hsa00360	Phenylalanine metabolism	0.029	18	4
hsa00330	Arginine and proline metabolism	0.038	58	8
hsa_M00094	Ceramide biosynthesis	0.041	12	3

Table S1. Related to Figure 1.
Genes selectively (FDR<0.05) expressed in brite (1,691 genes) and white (1,138 genes) hMADS adipocytes at day 19 were subjected to functional enrichment analyses using Homer (Heinz et al. 2010). Top scoring metabolic pathways extracted from the KEGG database (Kanehisa and Goto 2000; Kanehisa et al. 2014) are shown for brite-selective (top) and white-selective (bottom) genes.

Loft et al._Figure S1

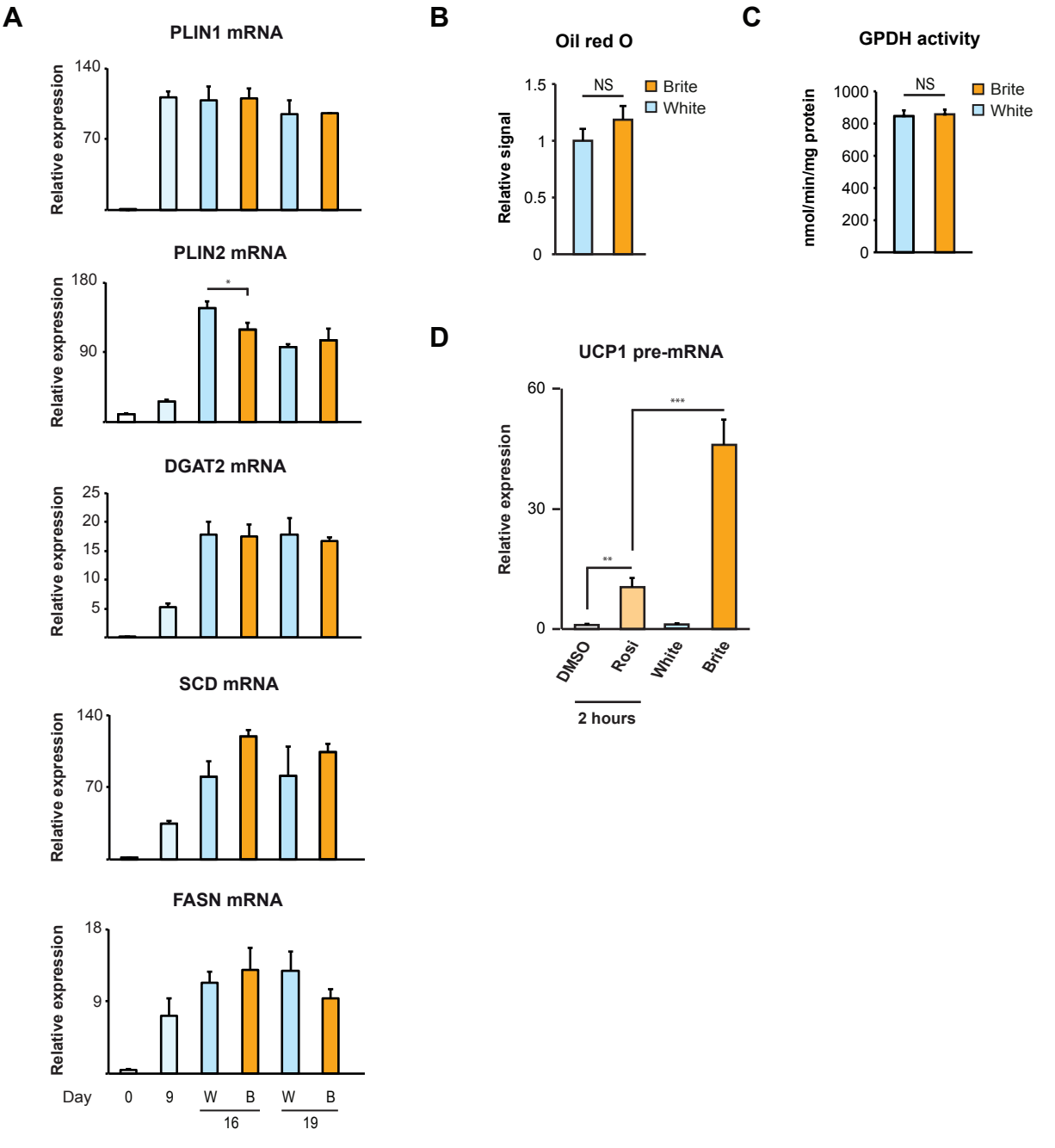

Figure S1. Related to Figure 1.

A. mRNA expression of the general adipocyte marker genes, perilipin 1 (*PLIN1*), *PLIN2*, diacylglycerol O-acyltransferase 2 (*DGAT2*), stearoyl-CoA desaturase (*SCD*), and fatty acid synthase (*FASN*) was determined during hMADS differentiation at the indicated time points. Error bars represent S.D. (n=3). p-values: **<0.005 as indicated. W=White, B=Brite.

B. Quantification of lipids in white and brite hMADS adipocytes. White (light blue) and brite (orange) hMADS adipocytes were fixed with formaldehyde and stained with oil red O. The dye retained by the lipid vacuoles was quantified by measuring optical density at 500 nm by spectrophotometric analysis. Error bars represent S.E.M. (n=4). NS=not significant (p>0.05).

C. Glycerol-3-phosphate dehydrogenase (GPDH) activity was determined in white (light blue) and brite (orange) hMADS adipocytes. Error bars represent S.E.M. (n=4). NS=not significant (p>0.05).

D. UCP1 transcription is acutely induced by rosiglitazone at day 13, but requires long-term exposure to rosiglitazone for full activation. UCP1 pre-mRNA levels were determined following 2 hours exposure to DMSO (white) or rosiglitazone (light orange) at day 13 as well as in day 19 white (light blue) and brite (orange) adipocytes. Error bars represent S.D. (n=3). p-values: ***<0.001, **<0.005 as indicated.

Loft et al._Figure S2

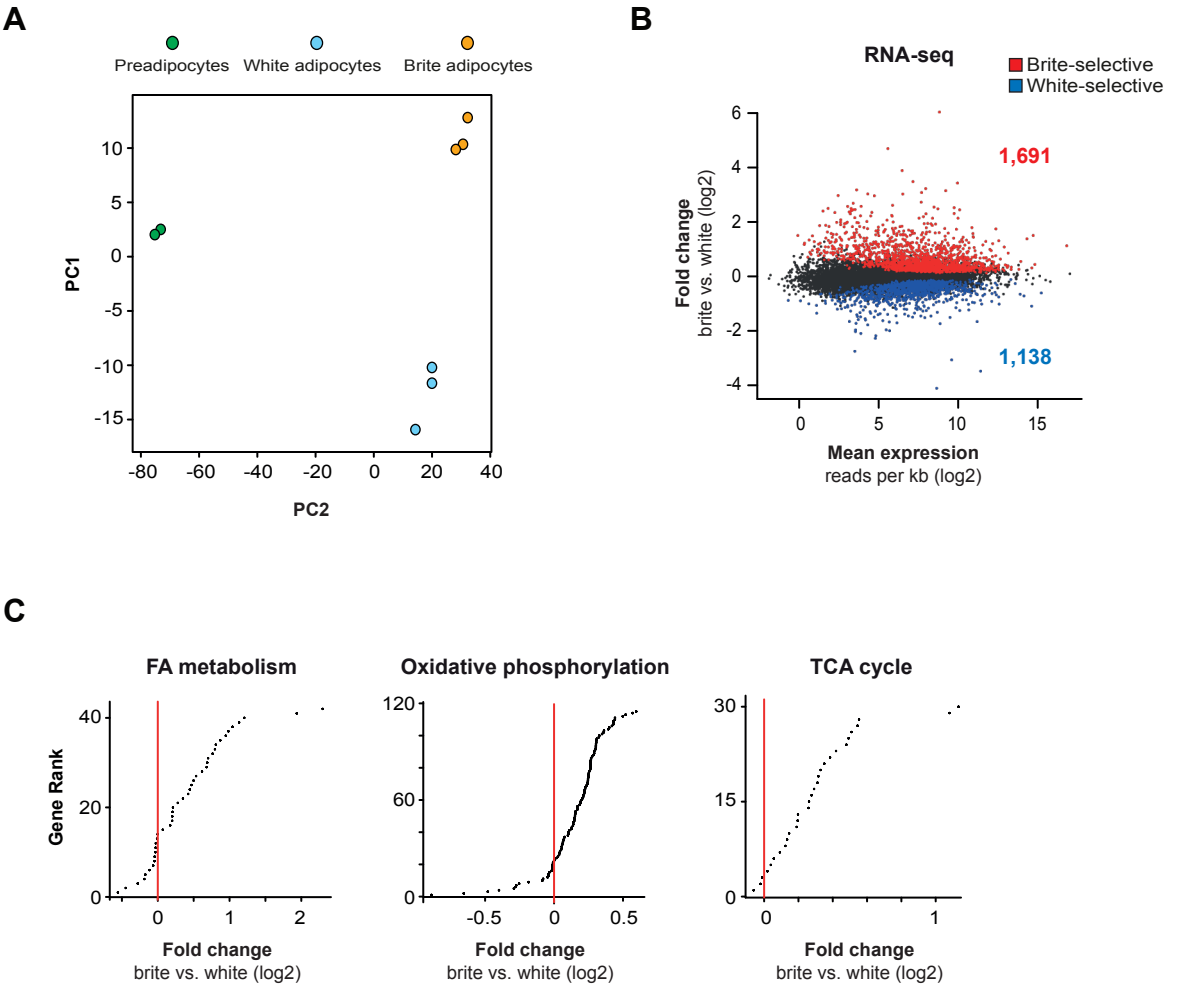

Figure S2. Related to Figure 1.

A. Principal component analysis of the top 500 genes with lowest variance in the respective RNA-seq duplicates from hMADS preadipocytes (green) as well as RNA-seq triplicates from white (light blue) and brite (orange) hMADS adipocytes at day 19.

B. MA-plot comparing RNA expression in brite and white adipocytes. The plot shows mean expression (as normalized exon reads per kilobase) of all 13,307 expressed genes versus the log2 fold change for a given gene transcript in brite compared to white hMADS adipocytes at day 19. Significant (FDR<0.05) white-selective (blue, 1,138) and brite-selective (red, 1,691) genes are indicated.

C. Genes belonging to fatty acid metabolism, oxidative phosphorylation and TCA cycle display elevated expression levels in brite compared to white adipocytes. Metabolic pathways were extracted from the KEGG database (Kanehisa and Goto 2000; Kanehisa et al. 2014). For these pathways the mean log2 fold change in expression values for brite versus white hMADS adipocytes is plotted as a function of their gene rank.

Loft et al._Figure S3

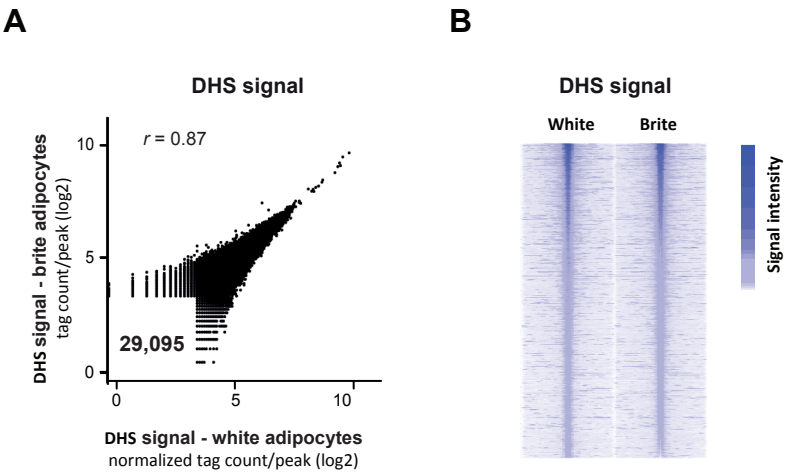

Figure S3. Related to Figure 2.

A. Scatterplot showing DHS tag counts (400 bp window) in all identified DHS sites (29,095 sites) in white and brite hMADS adipocytes at day 19. *r* indicates Pearson's correlation coefficient.

B. Heat map showing DHS signal intensity in a ±2-kb window around all DHS peak centers in white and brite hMADS adipocytes at day 19.

Loft et al._Figure S4

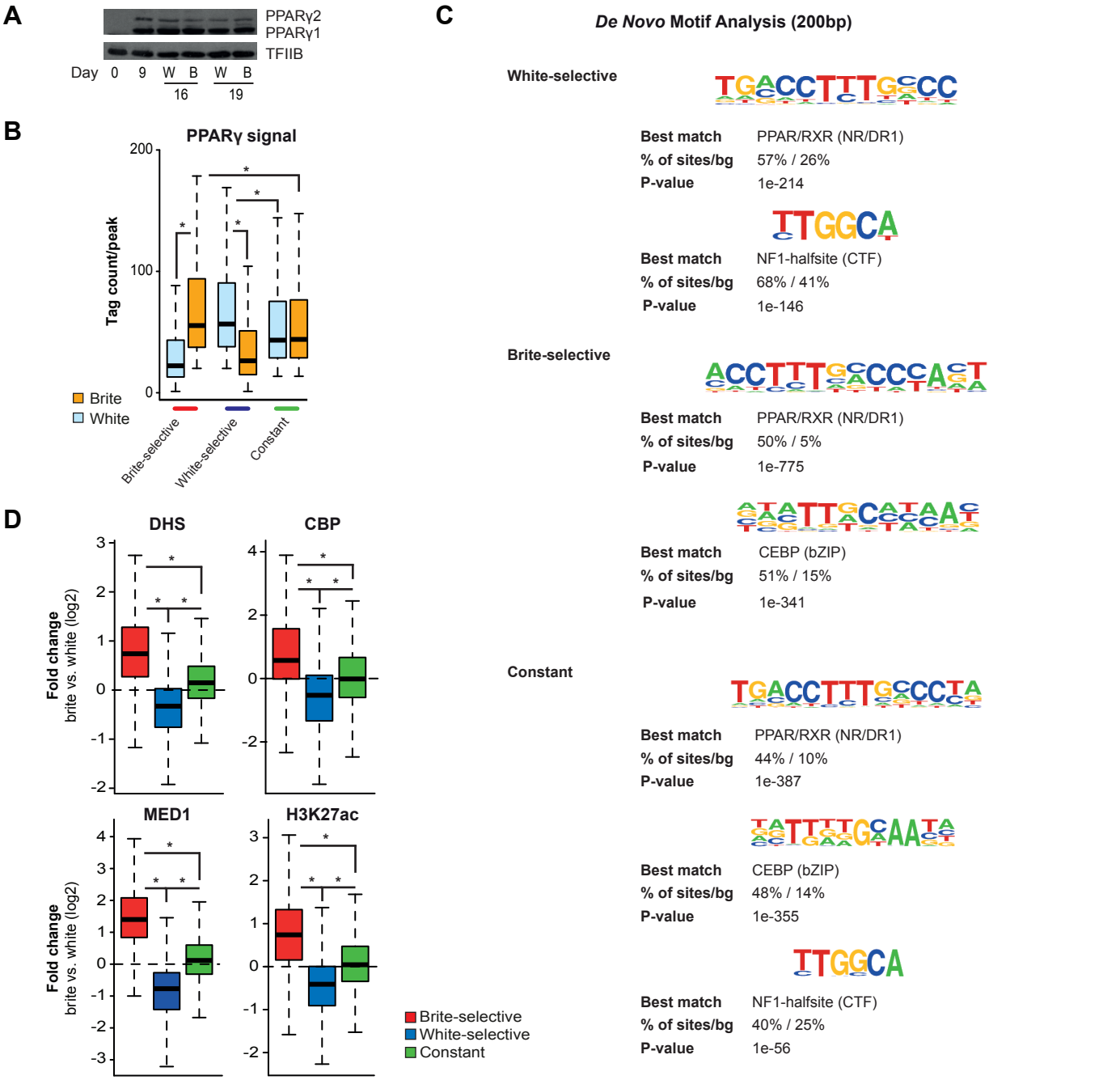

Figure S4. Related to Figure 2.

A. Western blot showing PPARγ protein expression during hMADS differentiation at the indicated days. W=White, B=Brite.

B. PPARγ signal (as tag count per peak in a 400 bp window) in PPARγ binding sites that are brite-selective (red, 2,211 peaks), white-selective (blue, 2,228 peaks) or constant (green, 2,385 peaks) in white (light blue) and brite (orange) hMADS adipocytes. p-value: *<2.2e-16 as indicated, Wilcoxon rank sum test.

C. Top scoring motifs from *de novo* motif analyses of 200bp regions centered around PPARγ binding sites that are brite-selective, white-selective, or constant. The % of target sites (sites) as well as % of background sites (bg) with the given motif is displayed. RXR = retinoid X receptor, NR=nuclear receptor, DR1 = direct repeat 1, NF1 = nuclear factor 1, CTF = CAAT-binding transcription factor, CEBP = CCAAT/Enhancer Binding Protein, bZIP = basic leucine zipper.

D. Boxplot showing the log2 fold change in DHS, CBP, MED1, and H3K27ac signal in PPARγ binding sites that are brite-selective (red), white-selective (blue), or constant (green). DHS, CBP, and MED1 signals were counted in a 400 bp window and H3K27ac signal in a 2kb window around the PPARγ peak center. p-value: *<2.2e-16 as indicated, Wilcoxon rank sum test.

Loft et al._Figure S5

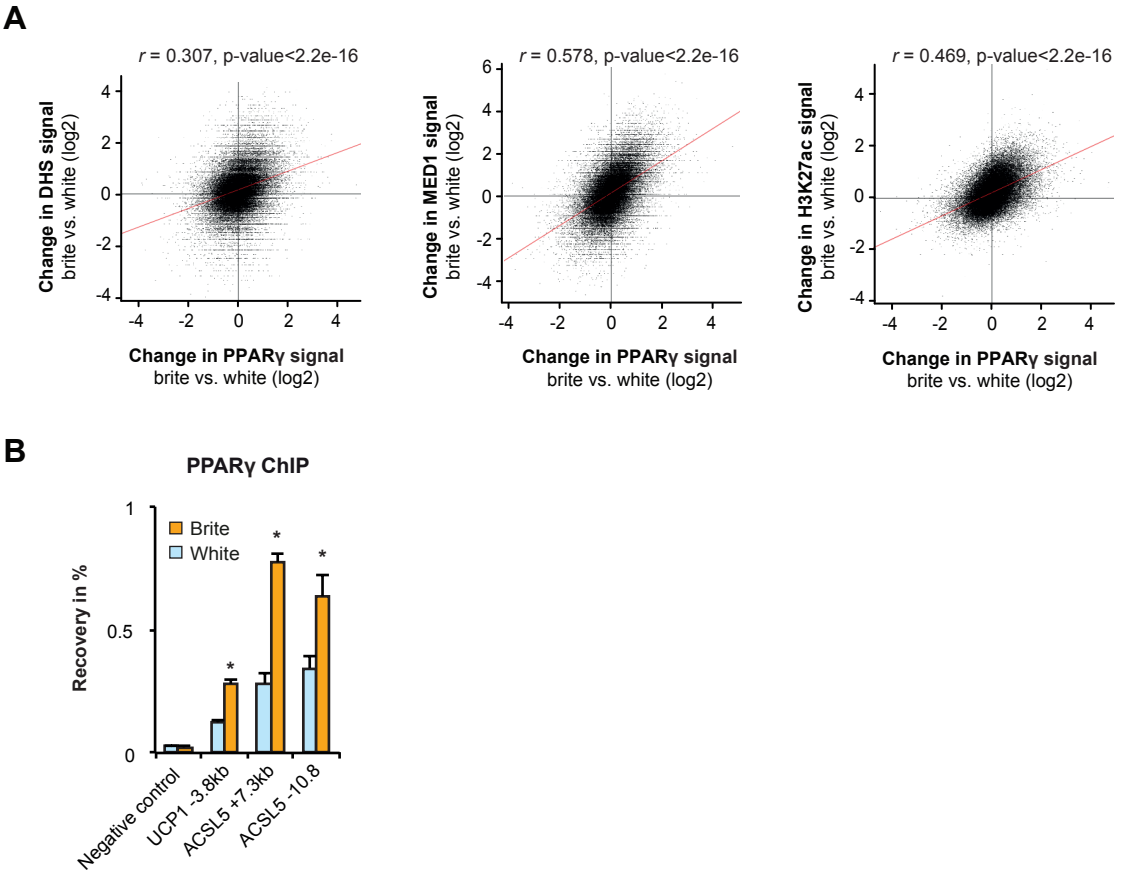

Figure S5. Related to Figure 2.

A. Correlation between log2 fold change in PPARγ signal and DHS (left), MED1 (middle), and H3K27ac (right) signal in brite compared to white hMADS adipocytes at all identified PPARγ binding sites (52,030). *r* indicates Pearson's correlation coefficient and the red line shows the linear regression between plotted values.

B. Brite-selective PPARγ binding sites shown in figure 2D (*UCP1* -3.8kb, *ACSL5* -10.8kb and +7.3kb) were validated by ChIP-qPCR in white (light blue) and brite (orange) hMADS adipocytes and expressed as % recovery compared to input sample. A negative control region (without any binding of PPARγ) is included. Error bars represent S.E.M. (n=3). *<0.05 in brite compared to white hMADS adipocytes.

Loft et al._Figure S6

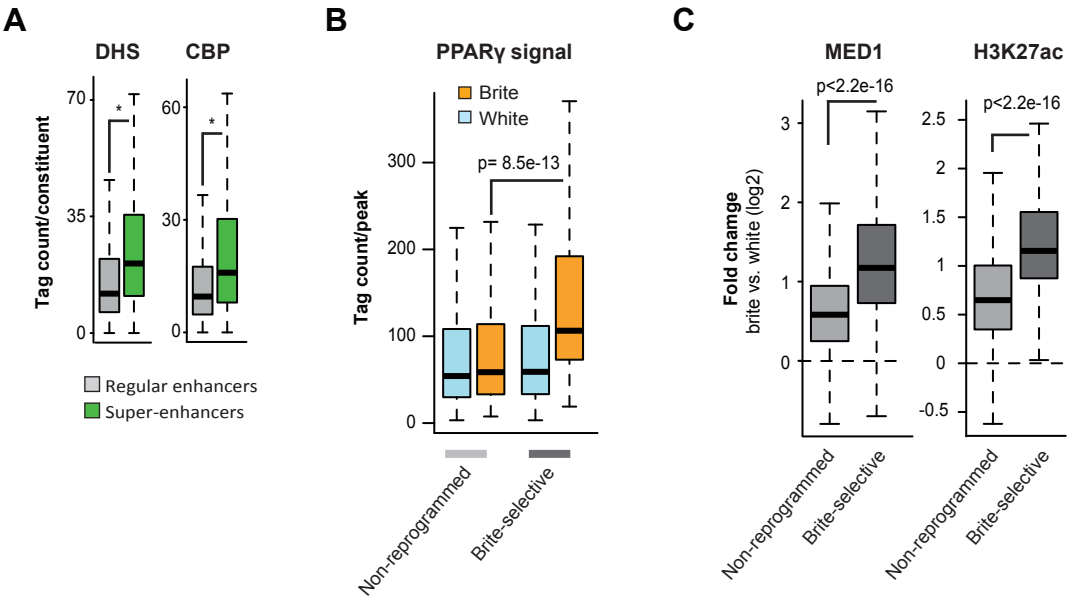

Figure S6. Related to Figure 3.

A. DHS and CBP signal (as tag count per peak in a 400bp window) in PPARγ constituents in regular PPARγ binding regions (grey, 46,392 peaks) and PPARγ super-enhancers (green, 5,638 peaks) in brite hMADS adipocytes. p-value: *<2.2e-16 as indicated, Wilcoxon rank sum test.

B. PPARγ signal (as tag count per peak in a 400bp window) in non-reprogrammed (light grey, 1,296 peaks) or brite-selective (dark grey, 139 peaks) PPARγ constituents within brite-selective PPARγ super-enhancers in white (light blue) and brite (orange) hMADS adipocytes. p-value was determined by Wilcoxon rank sum test.

C. Boxplot showing the log2 fold change in MED1 (400bp window) and H3K27ac signal (2kb window) in non-reprogrammed (light grey, 1,296 peaks) or brite-selective (dark grey, 139 peaks) PPARγ constituents within brite-selective PPARγ super-enhancers in brite compared to white hMADS adipocytes. p-value was determined by Wilcoxon rank sum test.

Loft et al._Figure S7

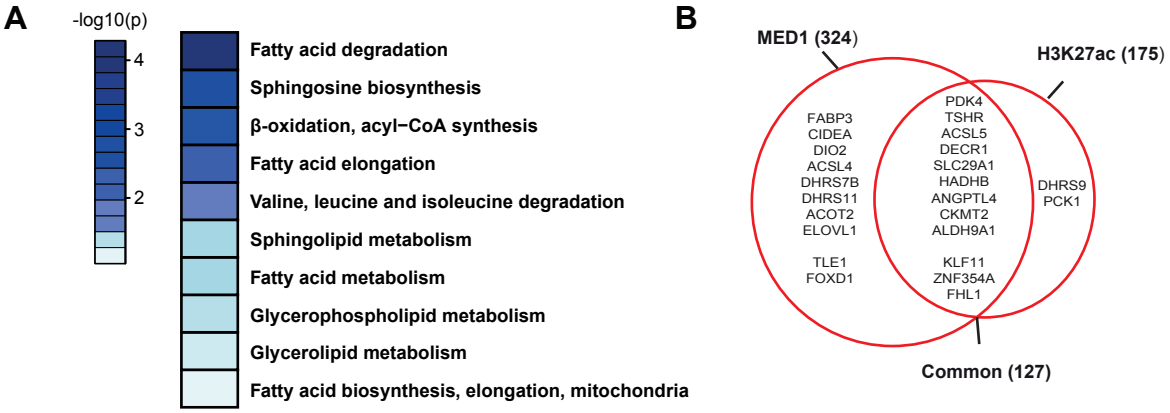

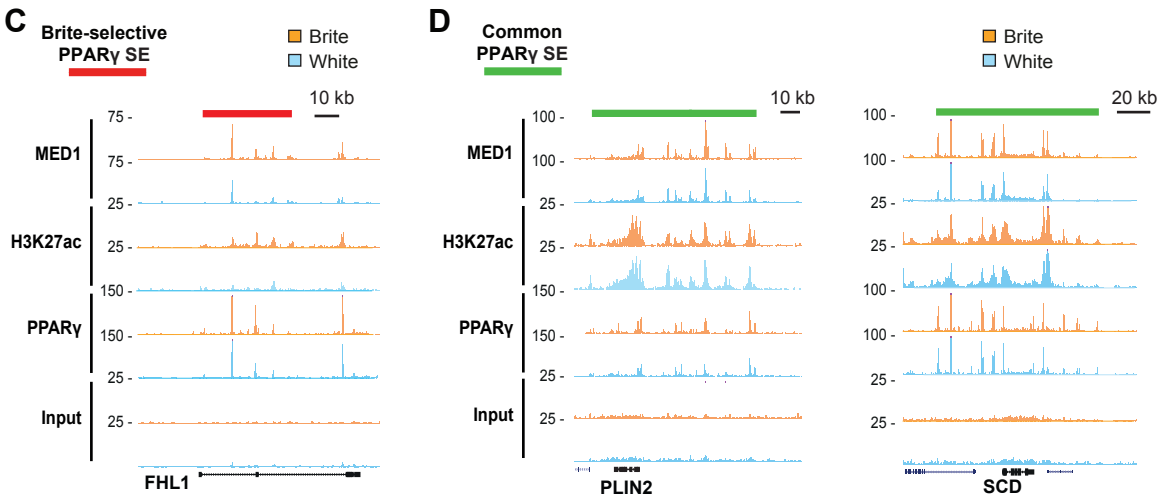

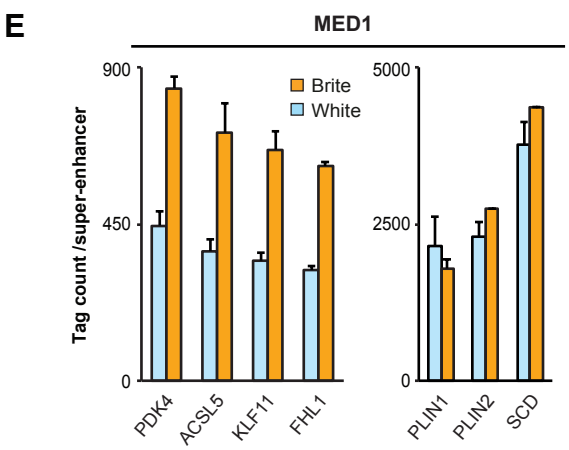

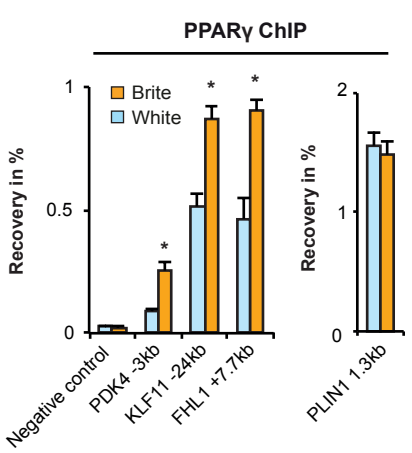

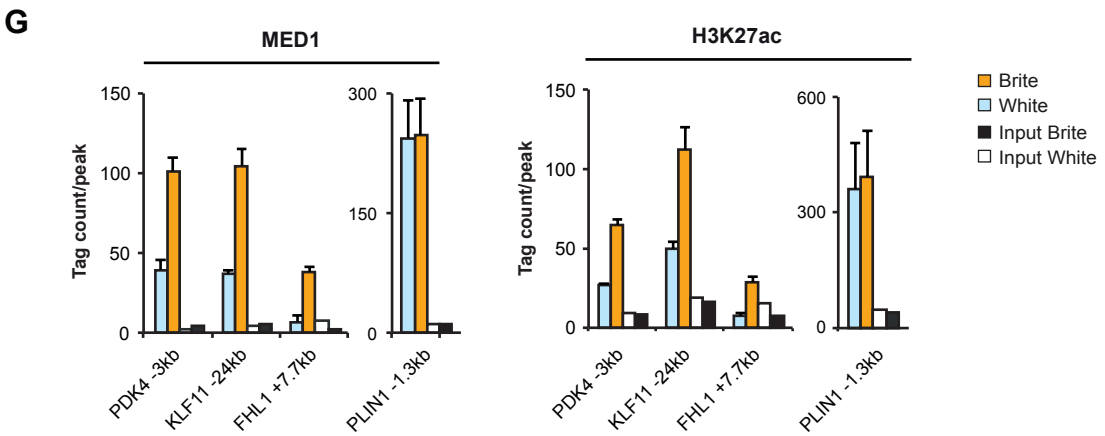

Figure S7. Related to Figure 3.

A. Functional enrichment analysis of genes associated with brite-selective super-enhancers using HOMER (Heinz et al. 2010). Top scoring metabolic pathways extracted from the KEGG database (Kanehisa and Goto 2000; Kanehisa et al. 2014) are shown with p-values as illustrated in the heatmap.

B. Overlap between brite-selective PPARγ super-enhancers (SE) as determined by MED1- (324 regions) and H3K27ac-ranking (175 regions). A subset of brite-selective genes associated to the brite-selective PPARγ super-enhancers is listed.

C+D. ChIP-seq profiles of PPARγ, H3K27ac, and input control at the *FHL1* (C) and *PLIN2* and *SCD* (D) loci in white (light blue) and brite (orange) hMADS adipocytes. The red and green lines indicate the position of brite-selective and common PPARγ super-enhancers, respectively.

E. Bar plots showing mean tag count in the indicated PPARγ super-enhancer regions for duplicate MED1 ChIP-seq libraries in white (light blue) and brite (orange) hMADS adipocytes. Error bars represent S.E.M. (n=2).

F. Quantification of PPARγ binding to constituent binding sites within brite-selective PPARγ super-enhancers associated with the brite-selective genes *PDK4*, *KLF11*, and *FHL1* (left) as well as within a common super-enhancer associated to the general adipocyte gene *PLIN1* (right). Binding is determined by ChIP-qPCR in white (light blue) and brite (orange) hMADS adipocytes and expressed as % recovery compared to input sample. A negative control region (without any binding of PPARγ) is included. Error bars represent S.E.M. (n=3). *<0.05 in brite compared to white hMADS adipocytes.

G. Bar plots showing binding of MED1 (left) and association with H3K27ac (right) for the selected subset of PPARγ binding sites within super-enhancers shown in Figure S7F. MED1 (400 bp window) and H3K27ac (2kb window) signal (as tag count per peak) are derived from duplicate ChIP-seq libraries from white (light blue) and brite (orange) hMADS adipocytes. The input signal from white (white) and brite (black) hMADS adipocytes in the given window is plotted as a control. Error bars represent S.E.M. (n=2).

Loft et al._Figure S8

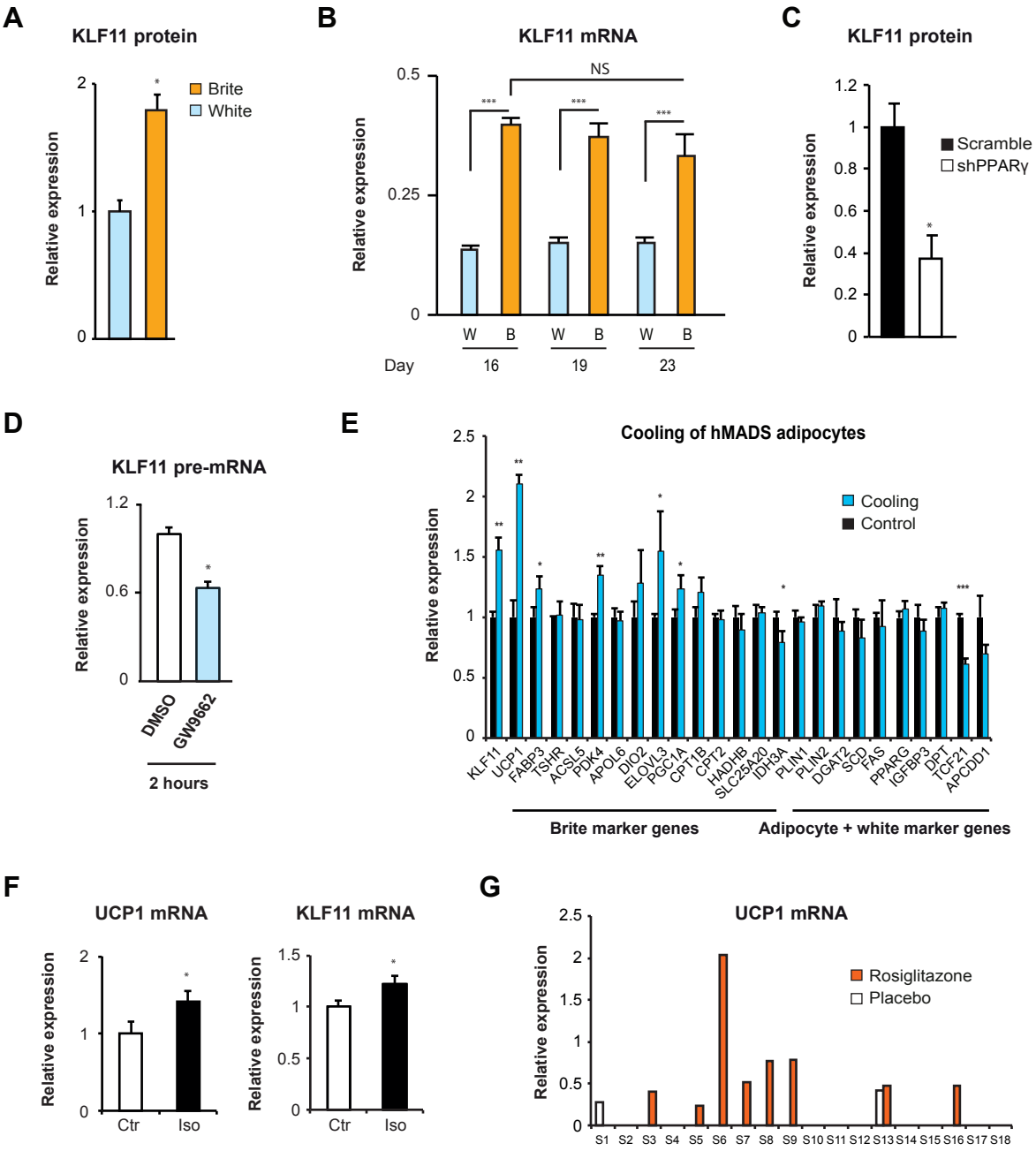

Figure S8. Related to Figure 4.

A. Densitometry scanning of KLF11 protein expression in white (light blue) and brite (orange) hMADS adipocytes at day 19. Protein data are normalized to SP1 expression. Error bars represent S.E.M. (n=3). p-values: *<0.05 compared to white adipocytes.

B. Expression of KLF11 mRNA in white (W, light blue) and brite (B, orange) hMADS adipocytes at the indicated time points. Error bars represent S.D. (n=3). p-values: ***<0.001, NS=not significant (p>0.05), as indicated.

C. Effect of PPARγ knockdown on KLF11 protein levels in hMADS adipocytes as in Figure 4C. hMADS adipocytes were transduced with lentivirus expressing scramble (black) or PPARγ (white) shRNA at day 10, and subsequently treated with rosiglitazone from day 13-16. KLF11 protein levels were determined by densitometry scanning and normalized to TFIIB expression. Error bars represent S.E.M. (n=3). p-values: *<0.05 compared to scramble control.

D. Effect of PPARγ antagonist on KLF11 transcription (as determined by pre-mRNA levels) in brite hMADS adipocytes at day 19. Cells were treated for 2 hours with DMSO (white) or the PPARγ antagonist GW9662 (light blue). Error bars represent S.D. (n=3). p-values: *<0.05 compared to DMSO control.

E. Effect of 4 hours of cooling on gene expression in brite hMADS adipocytes at day 19. Expression of brite and white marker genes as well as general adipocyte genes (same genes as in Figure 1F) is shown. Cooling was performed at 31°C (blue) and control cells were left at 37°C (black). Error bars represent S.E.M. (n=3). p-values: **<0.005, *<0.05 compared to control cells.

F. Effect of isoproterenol on UCP1 and KLF11 mRNA levels in brite hMADS adipocytes at day 19. Adipocytes were subjected to 6 hours treatment with vehicle (Ctr, black) or 1uM isoproterenol (Iso, white). Error bars represent S.E.M. (n=3). p-values: *<0.05 compared to control.

G. Relative expression of UCP1 in human subcutaneous abdominal WAT from a total of 18 subjects treated for 3 months with placebo (white) and then 3 months with rosiglitazone (red) or vice versa. mRNA expression was normalized to control genes, PPIA and PGK1. Details on the human cohort are previously described (Tan et al. 2005).

Loft et al._Figure S9

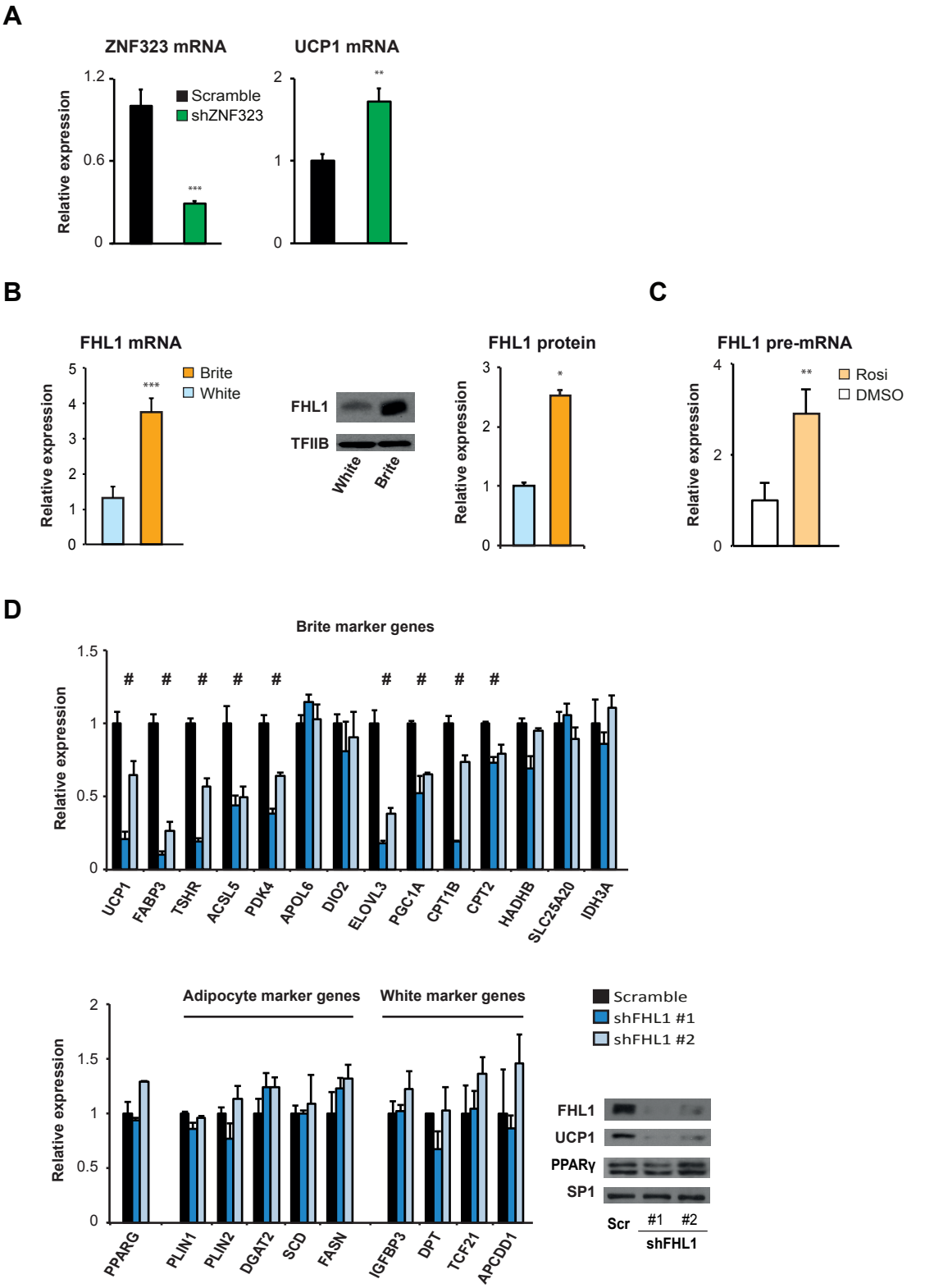

Figure S9. Related to Figure 5.

A. Effect of ZNF323 knockdown on expression of ZNF323 and UCP1 mRNA in day 16 hMADS adipocytes. hMADS adipocytes were transduced with lentivirus expressing scramble (black) or ZNF323 (green) shRNA at day 10, and subsequently treated with rosiglitazone from day 13-16. Error bars represent S.D. (n=3). p-value: ***<0.001, **<0.005 compared to scramble control.

B. FHL1 mRNA (left) and protein (middle and right) expression levels in white (light blue) and brite (orange) hMADS adipocytes at day 19. FHL1 protein levels were determined by densitometry scanning and normalized to TFIIB expression. Error bars represent S.E.M. (n=3). p-value: ***<0.001, *<0.05 compared to white adipocytes.

C. Effect of rosiglitazone on transcription of FHL1 (as determined by pre-mRNA levels) in hMADS adipocytes. hMADS adipocytes at day 13 were treated for 2 hours with DMSO (white) or rosiglitazone (light orange). p-value: **<0.005 compared to DMSO control.

D. Effect of FHL1 knockdown on rosiglitazone-induced browning. hMADS adipocytes were transduced with lentivirus expressing scramble (black) or one of two different FHL1 (blue) shRNAs at day 10, and subsequently treated with rosiglitazone from day 13-16. mRNA expression of brite, white and general adipocyte markers was determined on day 16. Error bars represent S.D. (n=3). p-value: #<0.02 for both lentiviral constructs compared to scramble control.

Loft et al._Figure S10

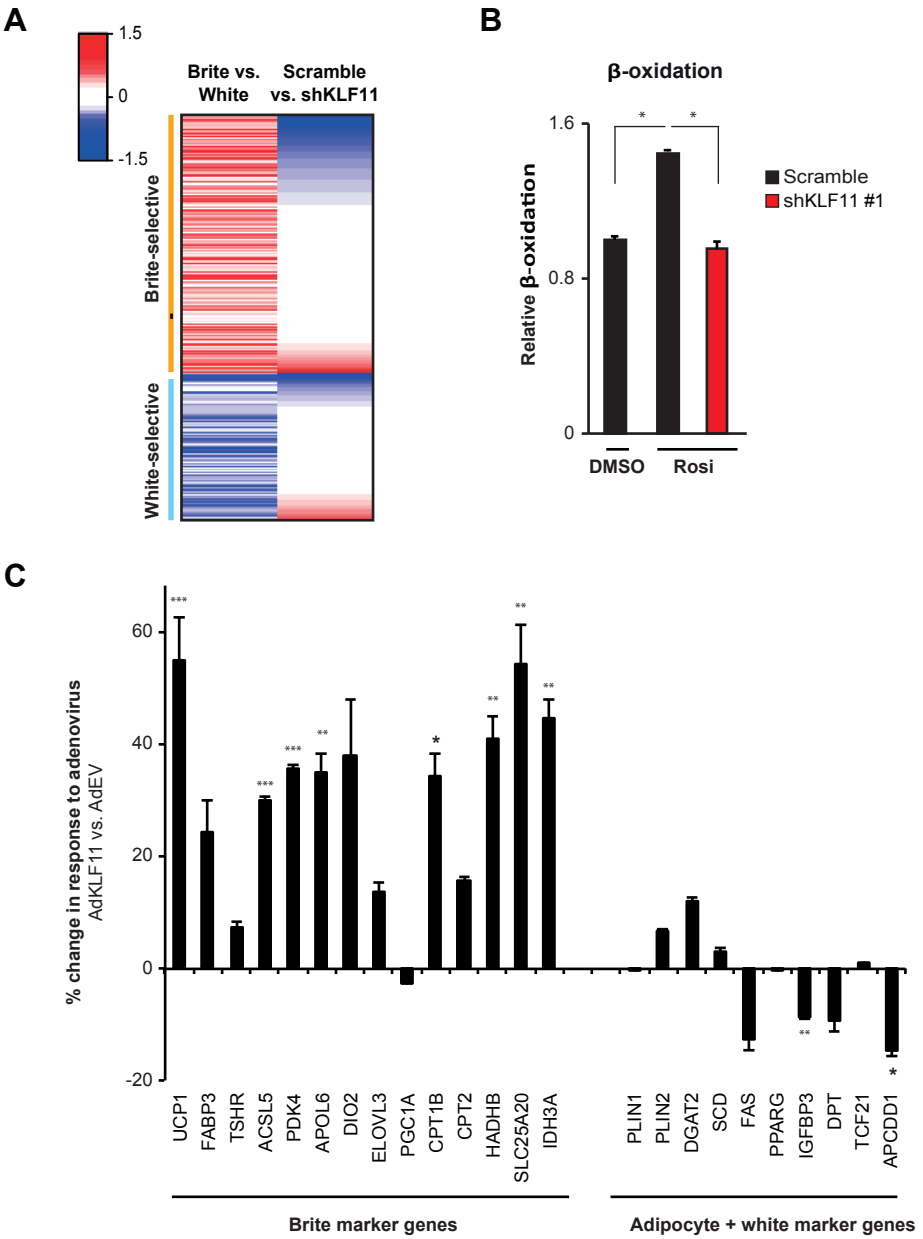

Figure S10. Related to Figure 5.

A. Effect of KLF11 knockdown on expression of white- and brite-selective genes in hMADS adipocytes. Heat map depicts the log2 fold changes in gene expression for white- and brite-selective genes in hMADS adipocytes. hMADS adipocytes were transduced with lentivirus expressing scramble or KLF11 shRNA at day 10, and subsequently exposed to rosiglitazone from day 13-16. RNA-seq was performed at day 16. Data for the knockdown experiments are presented as mean of two independent RNA-seq replicates.

B. Effect of KLF11 knockdown on β-oxidation in hMADS adipocytes. hMADS adipocytes were transduced with lentivirus expressing scramble (black) or KLF11 (red) shRNA at day 10, and subsequently exposed to DMSO or rosiglitazone from day 13-16. β-oxidation was assessed by measuring relative amounts of ^{14}C liberated from [1-^{14}C] oleate by scintillation counting. Error bars represent S.E.M. (n=3). p-value: *<0.05 as indicated.

C. Effect of ectopic expression of KLF11 on brite and white marker genes as well as general adipocyte markers in hMADS adipocytes. Rosiglitazone-treated hMADS adipocytes (day 15) were subjected to KLF11 adenovirus (AdKLF11) or empty adenoviral control (AdEV) and mRNA expression was evaluated 24 hours post transduction. The bar diagram shows % change in mRNA expression in AdKLF11-treated compared to AdEV-treated cells for the same subset of genes examined in Figure 5A-B. Error bars represent S.E.M. (n=3). p-values: ***<0.001, **<0.005, *<0.05 for AdKLF11 compared to AdEV.

Loft et al._Figure S11

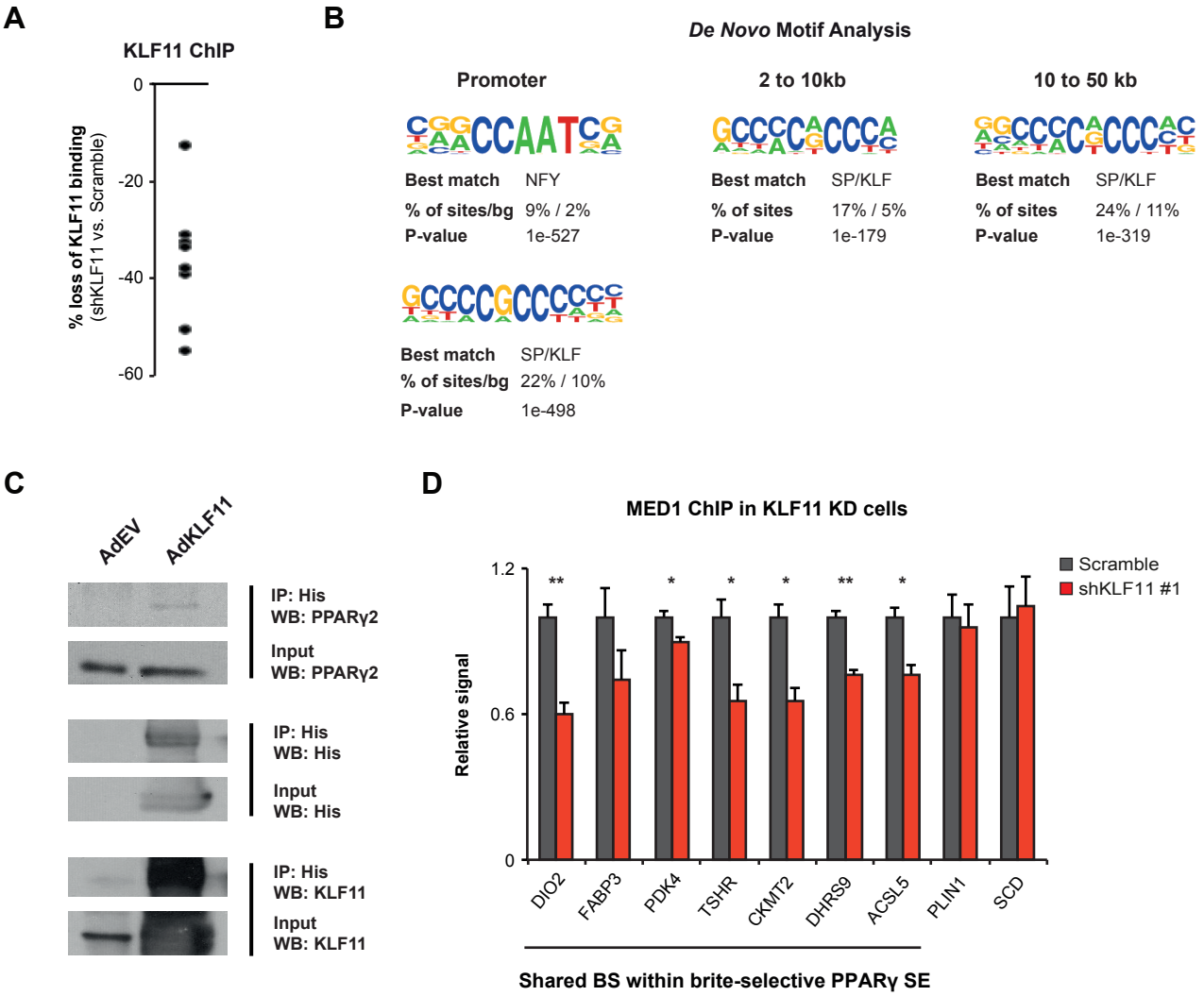

Figure S11. Related to Figure 6.

A. Plot illustrating the mean % loss of KLF11 (of 3 independent biological experiments) at selected target sites upon shRNA-mediated KLF11 knockdown in hMADS adipocytes.

B. Top scoring motifs from *de novo* motif analyses in 50bp regions around the center of KLF11 binding sites in the promoter region (16,390 sites within 2kb of TSS), near distal to genes (4,529 sites from 2kb to 10kb away from TSS) and far distal to genes (9,680 sites from 10kb to 50kb away from TSS). The % of target sites (sites) as well as % of background sites (bg) with the given motif is listed. NFY = nuclear transcription factor Y, SP = specificity protein, KLF = kruppel-like factor.

C. Co-immunoprecipitation of KLF11 and PPARγ in hMADS adipocytes. At day 15 rosiglitazone-treated hMADS adipocytes were transduced with his-tagged KLF11 (AdKLF11) or control (AdEV) adenovirus. IP was performed 24 hours post transduction, and subsequently protein expression of PPARγ, KLF11, and his-tagged KLF11 was examined by western blotting on immounoprecipitated and input material. Data are representative of two independent experiments.

D. Effect of KLF11 knockdown on relative MED1 occupancy at a subset of shared PPARγ/KLF11 binding sites (BS) within brite-selective PPARγ super-enhancers. hMADS adipocytes were transduced with lentivirus expressing scramble (dark grey) or KLF11 (red) shRNA at day 10 and subsequently exposed to rosiglitazone from day 13-16. MED1 binding was determined by ChIP-qPCR at a subset of shared PPARγ/KLF11 binding sites (BS) within brite-selective PPARγ super-enhancers at day 16. Two shared PPARγ/KLF11 binding sites (*PLIN1* 1.3kb, and *SCD1* -12kb) within common PPARγ super-enhancers are shown for comparison. Error bars represent S.E.M. (n=3). p-values: **<0.005, *<0.05 for Scramble compared to shKLF11.

Loft et al._Figure S12

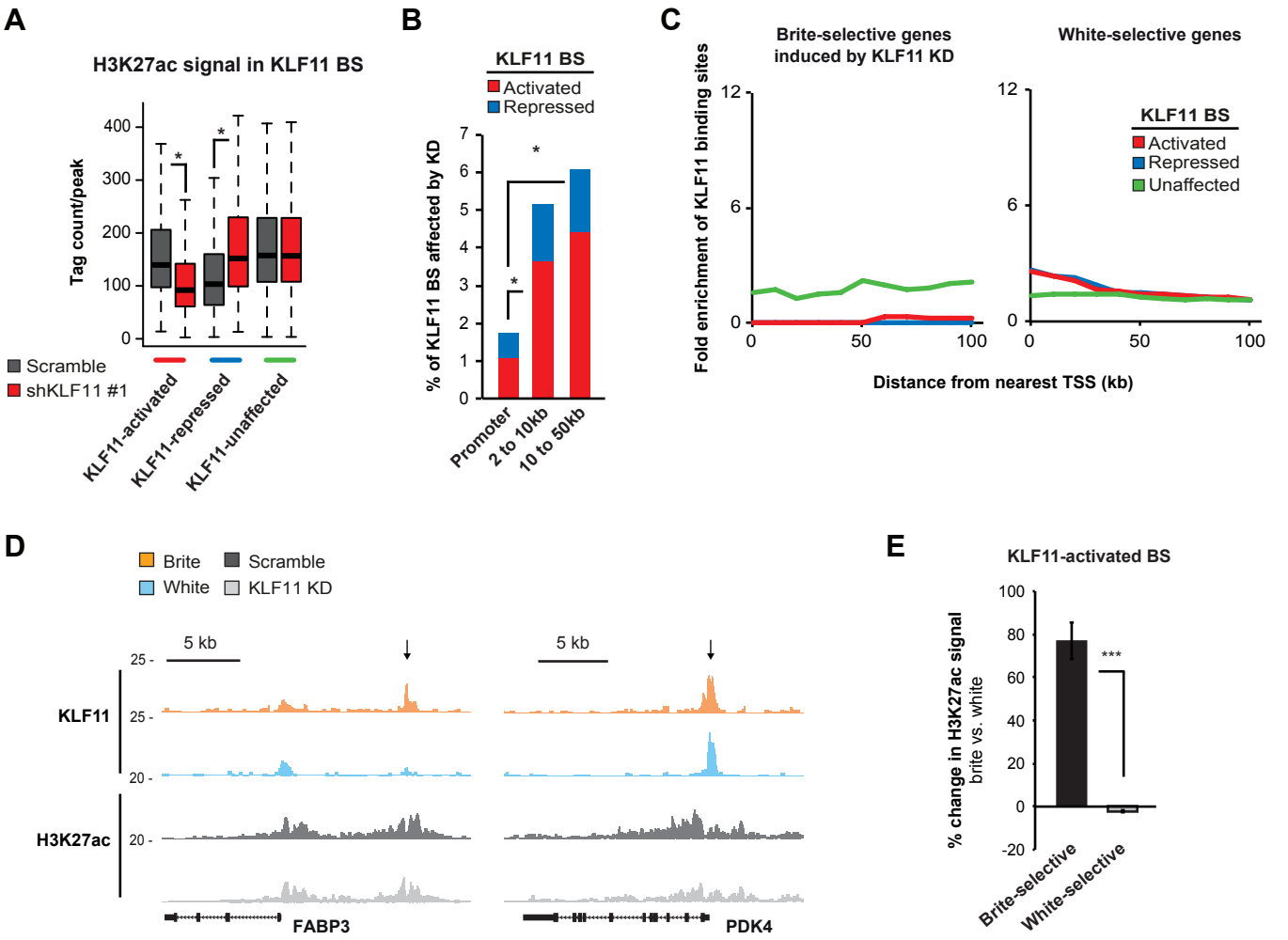

Figure S12. Related to Figure 6.

A. H3K27ac signal (as tag count per peak in a 2kb window) in putative KLF11-activated (red, 1,179 sites), KLF11-repressed (blue, 489 sites) and KLF11-unaffected (green, 1,076 sites) binding sites (BS). hMADS adipocytes were transduced with lentivirus expressing scramble (dark grey) or KLF11 (red) shRNA at day 10 and subsequently exposed to rosiglitazone from day 13-16. ChIP-seq was performed at day 16 in scramble and KLF11 knock down cells.

B. Plot showing the % of total KLF11 binding sites (BS) located in the promoter region (within 2kb of TSS), near distal (from 2kb to 10kb away from TSS) or far distal (10kb to 50kb away from TSS) regions that are activated (red) or repressed (blue) by KLF11 knockdown.

C. Enrichment of KLF11-activated (red), KLF11-repressed (blue), or KLF11-unaffected (green) binding sites (BS) near top brite-selective genes significantly induced by KLF11 knockdown (left) or top white-selective genes (right). Enrichment is determined as the number of binding sites per gene within different distances from the TSS (0-100 kb) of regulated genes relative to the number of binding sites per gene of constitutively expressed genes, as defined in Figure 1E.

D. ChIP-seq profiles of KLF11 in white (light blue) and brite (orange) hMADS adipocytes as well as H3K27ac profiles from the *FABP3* and *PDK4* loci in hMADS adipocytes transduced with Scramble (dark grey) or KLF11 #1 (light grey) shRNA. The arrows indicate putative KLF11-activated binding sites with loss of H3K27ac upon knockdown of KLF11.

E. Plot illustrating mean % change in H3K27ac signal in brite compared to white hMADS adipocytes at KLF11-activated binding sites within 100kb of top brite- (black) and white-selective (grey) genes. Error bars represent the 95% confidence interval around the mean. p-value: ***<0.001, two-tailed Student's test.

Supplemental Materials and Methods

hMADS cell culturing and differentiation

hMADS cells are self-renewing multipotent stem cells that exhibit a normal karyotype. The isolation and characterization of hMADS-3 cells obtained from the prepubic fat pad of a 4-month-old male donor have previously been reported (Rodriguez et al. 2004; Rodriguez et al. 2005). In this work hMADS-3 cells were cultured in DMEM (Lonza, low glucose) supplemented with 10% fetal bovine serum (Lonza), 10 mM Hepes, 2 mM L-glutamine (Lonza), penicillin (62.5 µg/ml), streptomycin (100 µg/ml), and 2.5 ng/ml hFGF2 (Peprotech). Two days post confluence (day 0) the cells were induced to differentiate in DMEM/Ham`s F12 (Lonza) supplemented with 10 µg/ml transferrin, 1 µM dexamethasone, 500 µM 3-isobutyl-1-methylxanthine (IBMX), 0.85 µM insulin, and 0.2 nM T_3. At day 3 of differentiation, IBMX and dexamethasone were omitted from the medium and 0.5 µM rosiglitazone was added until day 9 of differentiation leading to development of white hMADS adipocytes. For induction of browning 0.5 µM rosiglitazone was added again at day 13 and left on the cells until day 16. Control white adipocytes were treated with DMSO from day 13 to 16. From day 16 and forth the differentiation medium of both white and brite adipocytes was depleted for rosiglitazone.

Fatty acid oxidation

Determination of fatty acid oxidation was performed essentially as previously described (Berge et al. 2003). In brief, hMADS cells were seeded in 25 cm^2 flasks, and immediately prior to measurements the medium was changed to Roswell Park Memorial Institute medium (RPMI, Life Technologies) containing 2.5 mM glucose, 1% FBS and 0.5 mM L-carnitine. After 30 min of incubation, each flask was added 100 µL of hot oleate solution consisting of RPMI medium with 20 µg/mL fatty acid-free BSA, and 2.5 mM hot oleate stock (6.67 mg/mL oleate, 5.625 µCi/mL hot [1-^{14}C] oleate, 8% ethanol and 91.7 mM KOH). Flasks were sealed with a rubber stopper containing filter paper and incubated at 37°C. After 4 hours flasks were placed on ice and added 300 µL phenethylamine:methanol (1:1, v/v) to the filter paper and 200 µL 6M HCl to the media. The cultures were left at room temperature overnight for [^{14}C]CO_2 trapping. The filter papers were then transferred to vials with 8 mL scintillation fluid, and ^{14}C was measured by scintillation counting. Data are expressed as mean values ± SEM. Two-tailed Student's t-test was used to determine significance.

Mitochondrial respiration data analyses

For mitochondrial respiration analysis, hMADS cells were seeded in 24 multi-well plates (Seahorse) and differentiated and/or transduced as described previously. Oxygen consumption rate (OCR) of 16 or 19 day-old differentiated cells was determined using an XF24 Extracellular Flux Analyzer (Seahorse Bioscience). Uncoupled and maximal OCR was determined using oligomycin (1.2 µM) and FCCP (1 µM), respectively. Rotenone and Antimycin A (R&A; 1 µM each) were used to inhibit Complex I- and Complex III-dependent respiration, respectively.

Mitochondrial parameters displayed in histograms were measured independently for each well using the following formula: "basal mitochondrial respiration" = (basal–R&A); "uncoupled mitochondrial respiration" = ((oligomycin–R&A)/(basal–R&A)); "maximal mitochondrial respiration" = (FCCP-R&A). Data are expressed as mean values ± SEM. Two-tailed Student's t-test was used to determine significance.

Data Analyses

RNA-seq data
RNA reads were aligned to the human reference genome (version hg19) using Bowtie2 (Langmead and Salzberg 2012) with standard parameters. Splice-junction reads were handled by creation of a pseudo-splice genome, similar to the strategy utilized in RSEQTools (Habegger et al. 2011). Reads were filtered post-alignment for a MAPQ score greater than or equal to 30. The number of exon reads for all RefSeq genes were counted using Subread (Liao et al. 2013). Differential expression between three independent replicates of white and brite hMADS adipocytes (FDR<0.05), or between two independent replicates of scramble and KLF11 knockdown samples (FDR<0.1) was determined using the Wald test for the GLM coefficients in DESeq2 (paired analysis) (Love et al. 2014). For some analyses a subset of top brite- (603 genes) and white-selective (292 genes) genes were defined as those having FDR<0.001 and a log2 fold change>0.5 in either direction. Functional enrichment analysis was performed with HOMER (Heinz et al. 2010) using pathways related to metabolism from the KEGG annotation (Kanehisa and Goto 2000; Kanehisa et al. 2014)

Mapping of DHS-/ChIP-seq data
Sequence reads from PPARγ-, MED1-, CBP-, KLF11-, and H3K27ac ChIP-seq libraries as well as input- and DHS-seq libraries were trimmed and collapsed using FASTX-Toolkit **(http://hannonlab.cshl.edu/fastx_toolkit/)**. Bowtie (Langmead et al. 2009) was used to align each collapsed library to the human reference genome (version hg19) using the following parameters: '-m 3 –best –strata', with all other parameters default. In all cases, tag counts were normalized to 10M reads in all subsequent analyses, unless stated otherwise. PPARγ-, MED1-, KLF11-, and H3K27ac ChIP-seq experiments were performed in two independent biological replicates and sequenced independently.

Peak-calling
Regions enriched for PPARγ, KLF11 or DHS signal in white and brite hMADS adipocytes were identified using HOMER (Heinz et al. 2010) with the '-size given' and '-factor' settings and with all other parameters set at default. Subsequently, an additional stringency filter was applied, so only peaks >15 fold (PPARγ), >10 fold (DHS) or >5 fold (KLF11) over the matching input control were kept for further analyses. Merged peak files were generated from the individual PPARγ, KLF11 or DHS peak files if the center of two or more peaks were within 250 bp. Peaks from these merged peak files were only included if having more than 30 tags (PPARγ peak file), 15 tags (KLF11 peak file), and 10 tags (DHS peak file) per 10 M tags in a 400 bp window around the center of each merged peak. This resulted in merged peak files consisting of 52,030 PPARγ peaks, 38,391 KLF11 peaks, and 29,095 DHS peaks. HOMER was also used for counting tags at identified peak regions, annotating binding sites to RefSeq genes, and performing *de novo* motif search.

Identification of PPARγ super-enhancers
For identification of PPARγ super-enhancers individual PPARγ peaks were stitched together if they were within 12,500 bp, as previously described (Whyte et al. 2013). Sequence tag information for MED1 and input control were obtained in a window corresponding to the stitched PPARγ peak region. All identified PPARγ regions were then ranked according to increasing total MED1 ChIP-seq signal (with subtraction of input) in the given regions. Regions with more than 200 input-subtracted MED1 ChIP-seq tags per 10 M total reads in two independent MED1 ChIP-seq replicates were regarded as PPARγ super-enhancers. In total, 1,212 PPARγ super-enhancers

were identified in white and/or brite hMADS adipocytes, and these were tested for differential MED1 occupancy. Identical criteria were used to rank the PPARγ regions based on total (input-subtracted) ChIP-seq signal of H3K27ac resulting in identification of 1,188 PPARγ super-enhancers.

Differential signal intensity in PPARγ binding sites and super-enhancers
Differential signal intensity in PPARγ binding regions in white and brite hMADS adipocytes was determined using HOMER. First, annotatePeaks.pl with the '-noadj' option was used to count the number of raw tags in PPARγ binding regions in the given condition (without any normalization). Then getdifferentialpeaks.pl was run with the parameters '-peaks –batch', which calls on EdgeR (Robinson et al. 2010) to perform differential expression calculations with paired analysis. For this analysis the raw tag counts will be normalized based on the total library size for each condition in the given PPARγ binding regions. An FDR<0.1 was used to determine differential PPARγ occupancy in the PPARγ peak regions, whereas an FDR<0.01 was applied to test PPARγ regular and super-enhancers for differential MED1 or H3K27ac occupancy. For comparison, peak regions and PPARγ super-enhancers with insignificant changes were defined based on FDR and log2 fold changes as indicated in the text.

Identification of H3K27ac-responsive KLF11 binding sites
For identification of H3K27ac-responsive KLF11 binding sites H3K27ac ChIP-seq was performed in hMADS adipocytes transduced with lentivirus expression KLF11 or scramble shRNA. H3K27ac tag count information was obtained in all KLF11 binding sites in a 2,000 bp window around the KLF11 peak center. KLF11 binding regions with a H3K27ac-to-input ratio above 2.5 (23,032 sites) were tested for differential H3K27ac signal using getdifferentialpeaks.pl from HOMER with the following parameters '-peaks -dispersion 0.01', and were regarded as responsive to the KLF11 knockdown if obtaining p<0.1.

Significance calculations in box plots
The p-value for the difference between data in box plots was computed using Wilcoxon rank sum test (unmatched samples) or Wilcoxon matched pairs signed ranks test (matched samples).

Significance calculation between categorical variables
The p-value between data containing categorical variables was computed using either Fisher's exact test (for samples sizes <2000) or Chi-square with Yates' continuity correction (for samples sizes >2000).

Correlation analyses
Pearson's product-moment correlation coefficient was used to determine the linear correlation between two data sets.

Supplemental References

Berge K, Tronstad K, Bohov P, Madsen L, Berge R. 2003. Impact of mitochondrial beta-oxidation in fatty acid-mediated inhibition of glioma cell proliferation. *Journal of lipid research* **44**: 118-127.

Habegger L, Sboner A, Gianoulis TA, Rozowsky J, Agarwal A, Snyder M, Gerstein M. 2011. RSEQtools: a modular framework to analyze RNA-Seq data using compact, anonymized data summaries. *Bioinformatics* **27**: 281-283.

Heinz S, Benner C, Spann N, Bertolino E, Lin Y, Laslo P, Cheng J, Murre C, Singh H, Glass C. 2010. Simple combinations of lineage-determining transcription factors prime cis-regulatory elements required for macrophage and B cell identities. *Molecular cell* **38**: 576-589.

Kanehisa M, Goto S. 2000. KEGG: kyoto encyclopedia of genes and genomes. *Nucleic Acids Res* **28**: 27-30.

Kanehisa M, Goto S, Sato Y, Kawashima M, Furumichi M, Tanabe M. 2014. Data, information, knowledge and principle: back to metabolism in KEGG. *Nucleic Acids Res* **42**: D199-205.

Langmead B, Salzberg SL. 2012. Fast gapped-read alignment with Bowtie 2. *Nat Methods* **9**: 357-359.

Langmead B, Trapnell C, Pop M, Salzberg SL. 2009. Ultrafast and memory-efficient alignment of short DNA sequences to the human genome. *Genome Biol* **10**: R25.

Liao Y, Smyth GK, Shi W. 2013. The Subread aligner: fast, accurate and scalable read mapping by seed-and-vote. *Nucleic Acids Res* **41**: e108.

Love MI, Huber W, Anders S. 2014. Moderated estimation of fold change and dispersion for RNA-Seq data with DESeq2. *bioRxiv*.

Robinson MD, McCarthy DJ, Smyth GK. 2010. edgeR: a Bioconductor package for differential expression analysis of digital gene expression data. *Bioinformatics* **26**: 139-140.

Rodriguez A-M, Elabd C, Delteil F, Astier J, Vernochet C, Saint-Marc P, Guesnet J, Guezennec A, Amri E-Z, Dani C et al. 2004. Adipocyte differentiation of multipotent cells established from human adipose tissue. *Biochemical and biophysical research communications* **315**: 255-263.

Rodriguez A-M, Pisani D, Dechesne C, Turc-Carel C, Kurzenne J-Y, Wdziekonski B, Villageois A, Bagnis C, Breittmayer J-P, Groux H et al. 2005. Transplantation of a multipotent cell population from human adipose tissue induces dystrophin expression in the immunocompetent mdx mouse. *The Journal of experimental medicine* **201**: 1397-1405.

Tan GD, Fielding BA, Currie JM, Humphreys SM, Desage M, Frayn KN, Laville M, Vidal H, Karpe F. 2005. The effects of rosiglitazone on fatty acid and triglyceride metabolism in type 2 diabetes. *Diabetologia* **48**: 83-95.

Whyte WA, Orlando DA, Hnisz D, Abraham BJ, Lin CY, Kagey MH, Rahl PB, Lee TI, Young RA. 2013. Master transcription factors and mediator establish super-enhancers at key cell identity genes. *Cell* **153**: 307-319.